Kinetics of the Reaction of the $CHCl_2$ Radical with Oxygen Atoms

Stanislav I. Stoliarov,† Ákos Bencsura,‡ Eugene Shafir, Vadim D. Knyazev,* and Irene R. Slagle*

The Catholic University of America, Department of Chemistry, Washington, D.C. 20064.

Received: May 18, 2000; In Final Form: November 1, 2000

The kinetics of the reaction of $CHCl_2$ radical with $O(^3P)$ atoms has been studied in a heatable tubular reactor coupled to a photoionization mass spectrometer. The time-resolved decay of $CHCl_2$ was monitored as a function of O atom concentration (in a large excess of O atoms). The rate constants show a weak dependence on temperature over the 302−900 K range and can be represented by an Arrhenius expression $k(T) = k_3 = (9.00 \pm 0.92) \times 10^{-11}\exp(57.4 \pm 19.1\ \mathrm{K}/T)$ cm^3 molecule^{-1} s^{-1}. HCl was detected as a product of the $CHCl_2 + O(^3P)$ reaction.

I. Introduction

Because of the use of incineration as a treatment process for hazardous industrial wastes, including chlorinated hydrocarbons, kinetic modeling of chlorinated hydrocarbon combustion is an important field of research. Fundamental knowledge of mechanisms, specific pathways, and rate constants of important elementary reactions, including the reactions of chlorinated hydrocarbon radicals, is of key importance to the success of such modeling.

When compared to non-chlorinated alkyl radicals, alpha-chlorinated alkyl radicals are characterized by increased kinetic stability in the combustion environment due to weaker C−O bonds in the peroxy adducts formed by the addition of the radical to the O_2 molecule (see ref 1 and references therein). These weaker C−O bonds favor decomposition to O_2 and the chlorinated alkyl radical as opposed to further transformations of the adduct. Since high-temperature reactions between alpha-chlorinated alkyl radicals and O_2 are relatively slow, these radicals tend to accumulate in higher concentrations in flames resulting in a greater importance of their reactions with other open-shell species, such as OH, hydrocarbon radicals, and H atoms.[2] Reactions with O atoms can be expected to be important under fuel-lean conditions, where O atom concentrations are significant.

The only previously studied reactions of chlorinated alkyl radicals with O atoms are[3−5]

$$CCl_3 + O \rightarrow \text{products} \quad (1)$$

and

$$CH_2Cl + O \rightarrow \text{products} \quad (2)$$

Rate constants of both reactions exhibit similar weak negative temperature dependences, but the absolute values of the rate constants differ by a factor of 5.8: $k_1(298\ \mathrm{K}) = 4.5 \times 10^{-11}$ cm^3 molecule^{-1} s^{-1} while $k_2(298\ \mathrm{K}) = 2.6 \times 10^{-10}$ cm^3 molecule^{-1} s^{-1}. If these values are compared with that for the non-chlorinated methyl radical reaction with O atoms, 1.4×10^{-10} cm^3 molecule^{-1} s^{-1}, it can be seen that no apparent correlation between the number of Cl atoms at the radical center and the radical reactivity toward oxygen atoms can be derived. Similarly, no correlation exists with the ionization potential of the radical.[5] Therefore, direct experimental rate constant determination is the preferred method of assessing R + O reactivity for such systems.

In the current work, we report on the first direct experimental study of kinetics of the reaction between the $CHCl_2$ radical and $O(^3P)$ atoms:

$$CHCl_2 + O \rightarrow \text{products} \quad (3)$$

Section II describes the experimental method. The results are presented in section III. Discussion is presented in section IV and conclusion in section V.

II. Experimental Section

Details of the experimental apparatus[6] and procedures[4,5,7,8] used have been described before and so are only briefly reviewed here. Pulsed unfocused 193 nm radiation (∼4 Hz) from a Lambda Physic EMG 201MSC excimer laser was directed along the axis of a heatable quartz reactor (1.05 cm i.d.), which was uncoated or coated with boron oxide[9] to reduce the rates of heterogeneous reactions. The intensity of laser radiation inside the reactor was in the range 5−15 mJ pulse^{-1} cm^{-2}. Gas flowing through the tube at ∼4 m s^{-1} contained dichloroacetyl chloride ($CHCl_2$ radical precursor, $[CHCl_2C(O)Cl] = (0.5-2.5) \times 10^{12}$ molecules cm^{-3}), SO_2 (O atom precursor, $[SO_2] = (0.7-5.2) \times 10^{13}$ molecules cm^{-3}), and an inert carrier gas (helium) in large excess ($[He] = 12.0 \times 10^{16}$ molecules cm^{-3}, which corresponds to pressures of 3.75−11.18 Torr, depending on temperature). The flowing gas was completely replaced between laser pulses.

Gas was sampled through a hole (0.04 cm diameter) in the side of the reactor and formed into a beam by a conical skimmer before the gas entered the vacuum chamber containing the photoionization mass spectrometer. As the gas beam traversed the ion source, a portion was photoionized and mass selected. Temporal ion signal profiles were recorded on a multichannel

† Current address: University of Massachusetts, Department of Chemical Engineering, Amherst, MA 01003.

‡ Permanent address: Central Research Institute for Chemistry, Hungarian Academy of Sciences, P.O. Box 17, H-1525 Budapest, Hungary.

10.1021/jp0018293 CCC: $20.00
Published on Web 12/13/2000

TABLE 1: Conditions and Results of the Experiments to Measure k_3

T/K	[prec.][a]	$[CHCl_2]_0$[a]	$[SO_2]$[b]	$[O]_0$[c]	σ_{sys}[d]	σ_{stat}[d]	$k_6(\sigma)/s^{-1}$ [e]	$k_7(\sigma)/s^{-1}$ [e]	k'[f]	$\sigma(k')$[g]
302	14.75	0.71	2.135	33.34	0.96	1.38	63.1(11.6)	26.0(21.4)	467	82
302	11.70	0.68	1.420	21.34	0.68	0.97	69.7(7.0)	26.2(10.0)	336	57
302	12.20	0.68	1.665	29.75	1.09	1.19	55.2(11.5)	10.1(6.5)	393	55
302	9.08	0.47	0.938	17.88	0.43	0.67	69.5(9.1)	26.0(18.6)	321	60
302	5.43	0.30	0.680	11.51	0.39	0.42	57.0(18.2)	23.0(13.3)	182	54
			$k_3(T = 302\ K) = (1.41 \pm 0.17) \times 10^{-10}\ cm^3\ molecule^{-1}\ s^{-1}$ [h]							
500	17.35	0.97	1.955	30.35	1.88	0.36	3.7(2.1)	13.2(2.9)	341	19
500	9.16	0.51	0.792	14.33	1.69	0.15	5.0(5.9)	29.8(4.5)	190	16
500	11.50	0.47	1.390	22.15	1.02	0.35	5.9(1.6)	22.2(4.6)	238	13
500	11.45	0.62	2.280	41.12	1.78	0.45	6.8(2.8)	21.9(3.3)	501	26
500	6.51	0.365	0.836	14.52	0.66	0.21	3.3(3.5)	19.7(2.8)	175	14
500	25.15	0.54[i]	5.225	33.20	1.21	0.95	2.9(2.9)	12.9(1.9)	354	28
500	13.9	0.57	2.895	38.78	2.16	1.03	5.0(4.0)	14.3(2.2)	412	40
500	16.10	0.32[i]	2.970	20.72	0.47	0.51	1.8(2.3)	11.6(2.2)	216	18
500	22.15	0.45[i]	3.995	26.39	1.32	0.58	3.4(2.4)	12.6(3.4)	316	37
500	19.10	1.03	2.145	38.84	1.98	0.62	3.7(3.1)	11.4(2.2)	463	53
			$k_3(T = 500\ K) = (1.14 \pm 0.11) \times 10^{-10}\ cm^3\ molecule^{-1}\ s^{-1}$ [h]							
900[j]	5.08	0.24	1.480	26.59	0.14	0.40	1.4(1.5)	27.0(3.8)	271	12
900[j]	5.29	0.23	0.972	17.37	0.70	0.25	1.0(0.7)	34.7(5.7)	214	12
900[j]	6.07	0.32	1.945	34.40	1.07	0.45	2.3(1.5)	47.5(8.0)	366	25
900[j]	5.90	0.26	2.350	35.95	2.23	0.63	1.0(0.9)	53.4(7.6)	386	36
900[j]	7.42	0.36	2.085	34.39	2.90	0.45	2.6(2.5)	37.1(4.1)	368	20
			$k_3(T = 900\ K) = (1.06 \pm 0.07) \times 10^{-10}\ cm^3\ molecule^{-1}\ s^{-1}$ [h]							

[a] Concentration of the photolytic precursor of $CHCl_2$ ($CHCl_2C(O)Cl$) and upper limit to the initial concentration of the $CHCl_2$ radicals (as determined from the measured photolytic depletion of the precursor) in units of 10^{11} molecules cm^{-3}. [b] Concentration of $SO_2/10^{13}$ molecules cm^{-3}. [c] Initial concentration of O atoms/10^{11} molecules cm^{-3}. [d] Systematic and statistical (standard deviation) components of the uncertainty in $[O]_0/10^{11}$ molecules cm^{-3}. These (intermediate) measures of uncertainty in this and other parameters are cited in Table 1 for the purpose of analysis (see text). Final uncertainties in k_3 are cited as combinations of 2σ statistical and systematic uncertainties (see footnote "h"). [e] Values of k_6 and k_7 ($CHCl_2$ and O wall loss rates). Values in parentheses represent intermediate measures of uncertainties (standard deviations, see footnote "d") with variations of rate constant values during the experiment included (to be incorporated in $\sigma(k')$). [f] k' values in s^{-1} ($k' = k_3[O]_0$) obtained from fitting experimental $CHCl_2$ temporal decay profiles with eq I. [g] Measure of statistical uncertainty (standard deviation, see note d) of k' with effects of uncertainties in k_6 and k_7 included. [h] Reported uncertainties are sums of 2σ statistical and systematic uncertainties. [i] Photolyzing laser was attenuated with wire mesh (attenuation factor 2.6). [j] Uncoated quartz reactor was used. Quartz reactor coated with boron oxide was used in all other experiments.

scaler from a short time before each laser pulse up to 20−50 ms following the pulse. Data from 1000 to 61000 repetitions of the experiment were accumulated before the data were analyzed.

Reactants and products of the photolysis and the reaction under study were photoionized by using atomic resonance radiation. The following combinations of lamps and windows were used in this study: a neon lamp with collimated hole structure (16.7, 16.9 eV) for ionizing O, SO_2, and HCl; an argon lamp with LiF window (11.6, 11.8 eV) for ionizing CHClO, CCl_2, CCl_2O, and $CHCl_2C(O)Cl$; a hydrogen lamp with MgF_2 window (10.2 eV) for ionizing CHCl; and a chlorine lamp with CaF_2 window (8.9−9.1 eV) for ionizing $CHCl_2$. All species were detected at the m/z ratios corresponding to their parent ions.

The two reactants ($CHCl_2$ and O) were produced by the simultaneous laser photolysis of $CHCl_2C(O)Cl$ and SO_2:

$$CHCl_2C(O)Cl \xrightarrow{h\nu} CHCl_2 + \text{products} \qquad (4)$$

$$\xrightarrow{h\nu} \text{other products}$$

$$SO_2 \xrightarrow{h\nu} SO + O(^3P) \qquad (5)$$

193 nm photolysis of SO_2 (reaction 5) has been shown to be an excellent photolytic source of ground-state O atoms.[8] The only product of reaction 5, other than the O atom, is the SO molecule, which is significantly less reactive with hydrocarbon radicals than is the O atom (see further discussion in this section). The gases used were obtained from Matheson (SO_2, 99.98% min) and MG Industries (He, 99.999% min). Dichloroacetyl chloride was obtained from Aldrich (99%). SO_2 and $CHCl_2C(O)Cl$ were purified by vacuum distillation prior to use. Helium was used as provided.

The procedures used to measure radical + O rate constants have been published before.[4,5,7,8] Initial reaction conditions ($[O]_0$ and $[CHCl_2]_0$) were selected to yield a large excess of O atoms over $CHCl_2$ radicals, $[O]_0/[CHCl_2]_0 \geq 28$. These initial concentrations were determined from the measured extent of photolytic depletion of SO_2 (6−19%) and $CHCl_2C(O)Cl$ (2−6%), respectively. Photolytic depletion is defined as the fraction of substrate decomposed due to photolysis. At the highest temperature of the current study, 900 K, the signal of dichloroacetyl chloride was too weak (most likely due to ion fragmentation increasing with temperature) to measure its photolytic depletion. Therefore, $[CHCl_2]_0$ values at 900 K were estimated under the assumption that photolytic depletion of $CHCl_2C(O)Cl$ at this temperature is the same as at 500 and 302 K (where it was measured directly and shown to be temperature independent). Comparison of $CHCl_2^+$ ion signal amplitudes obtained at 900 K with those obtained at lower temperatures and the absence of any signs of radical recombination (low values of radical wall loss rates, see Table 1) indicate that the above assumption does not result in any significant overestimation of $[CHCl_2]_0$. Only an upper limit of the $CHCl_2$ concentration could be determined from the photolytic depletion of the precursor due to the unknown yield of $CHCl_2$ in reaction 4. The initial concentrations of $CHCl_2$ and other products of $CHCl_2C(O)Cl$ photolysis were kept low ($\leq 10^{11}$ molecules cm^{-3}) to ensure that reactions between radicals, including the $CHCl_2$ + $CHCl_2$ reaction, had negligible rates compared to that of the

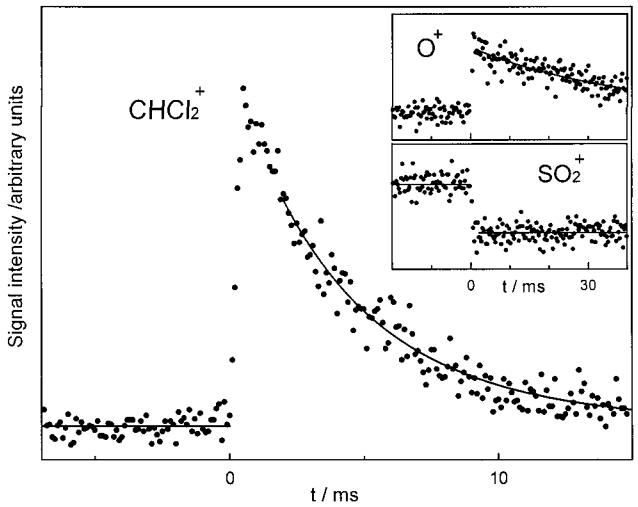

Figure 1. Examples of temporal ion signal profiles obtained in the experiments to measure k_3. $T = 500$ K, [He] $= 1.20 \times 10^{17}$ molecules cm^{-3}, [SO_2] $= 1.39 \times 10^{13}$, [$CHCl_2C(O)Cl$] $= 1.15 \times 10^{12}$, $[O]_0 = 2.22 \times 10^{12}$, $[CHCl_2]_0 \leq 4.7 \times 10^{10}$ molecules cm^{-3}, $k_7 = 22.2$ s^{-1}, $k' = 238$ s^{-1}. O^+ and SO_2^+ profiles presented were measured in steps 3 and 5 of the experimental procedure (see text).

reaction 3. Under the experimental conditions, the O atom concentration was not significantly depleted by the reaction under study or by any possible reactions between O and other products of dichloroacetyl chloride photolysis.

The following mechanism was used to analyze the observed kinetics of O atoms and $CHCl_2$ radicals:

$$CHCl_2 + O \rightarrow \text{products} \quad (3)$$

$$CHCl_2 \rightarrow \text{heterogeneous decay on the wall} \quad (6)$$

$$O \rightarrow \text{heterogeneous decay on the wall} \quad (7)$$

Within the above kinetic mechanism and under the conditions where O atoms are in large excess over the $CHCl_2$ radicals, the kinetics of $CHCl_2$ is given by the following expression:

$$[CHCl_2]_t = [CHCl_2]_0 \exp\left\{\frac{k'}{k_7}[\exp(-k_7 t) - 1] - k_6 t\right\} \quad \text{(I)}$$

where $k' = k_3[O]_0$.

Each experiment to determine k' consisted of the following sequence of kinetic measurements:

1. $CHCl_2$ decay due to heterogeneous loss, reaction 6 (only $CHCl_2C(O)Cl$ and He are present in the reactor). Determination of k_6.

2. Heterogeneous O atom decay due to reaction 7. (Temporal profile of O^+ at $m/z = 16$ is monitored; $CHCl_2C(O)Cl$, SO_2, and He are present in the reactor from step 2 to step 6 in this sequence.) Determination of k_7.

3. SO_2 depletion due to photolysis, reaction 5. Determination of $[O]_0$.

4. Decay of $CHCl_2$ due to reactions 3 and 6.

5. SO_2 depletion due to photolysis, reaction 5. Determination of $[O]_0$.

6. Heterogeneous O atom decay due to reaction 7 (repetition of step 2). Determination of k_7.

7. $CHCl_2$ decay due to heterogeneous loss, reaction 6 (only $CHCl_2C(O)Cl$ and He are present in the reactor). Determination of k_6.

Examples of experimentally obtained ion signal temporal profiles of SO_2, O, and $CHCl_2$ are presented in Figure 1.

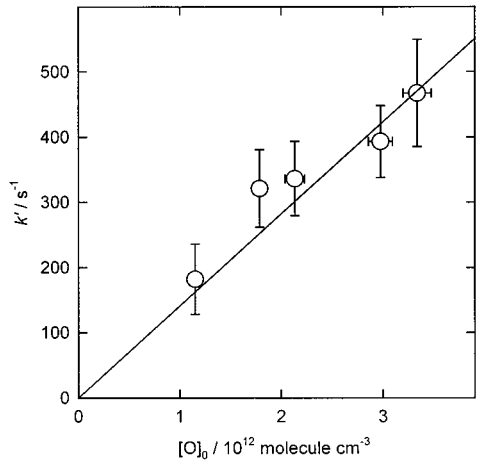

Figure 2. Dependence of k' on $[O]_0$ obtained at 302 K. Line is a linear fit. Error bars indicate the statistical components of uncertainties (standard deviation, see text). Initial O atom concentrations were obtained from photolytic depletion of SO_2 (see text, section II).

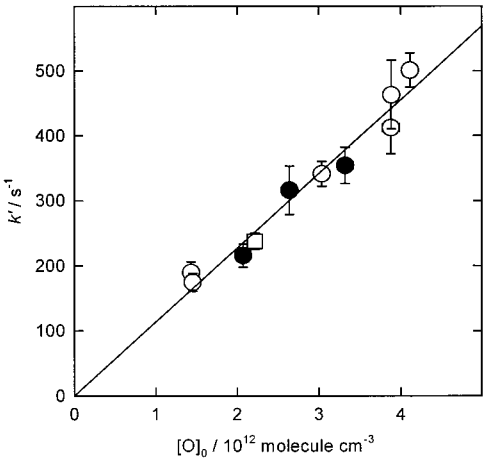

Figure 3. Dependence of k' on $[O]_0$ obtained at 500 K. Filled symbols, data obtained with the photolyzing laser attenuated by a factor of 2.6 with wire mesh; open symbols, data obtained with no laser attenuation. Line is a linear fit. Error bars indicate the statistical components of uncertainties (standard deviation, see text). Square represents the k' value obtained from the $CHCl_2$ profile in Figure 1.

The above sequence of measurements ensured reasonable stability of the heterogeneous wall loss rate constants and of the initial O atom concentration throughout the duration of the experiment. Any minor deviations between the values of these parameters obtained before and after the measurement of the $CHCl_2$ decay in entry number 4 were accounted for by taking the average of the two values and incorporating the deviations into the uncertainties. The k_6 and k_7 values thus obtained were used in fitting the experimental kinetics of the $CHCl_2$ radical (obtained in step 4) with expression I, which yielded the value of k'. The experiment was repeated several times with the O atom concentration varied (by changing the SO_2 concentration and/or attenuating the photolyzing laser radiation with wire mesh). Finally, the values of k_3 at each temperature were obtained from the slopes of linear k' vs $[O]_0$ dependences (Figures 2−4).

III. Results

Values of Rate Constants and Product Analysis. The conditions and results of all experiments are presented in Table 1 and k' vs $[O]_0$ dependences are shown in Figures 2−4. The absolute values of the rate constants of reaction 3 determined

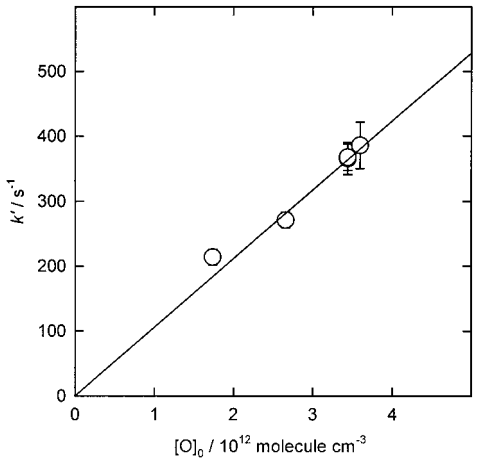

Figure 4. Dependence of k' on $[O]_0$ obtained at 900 K. Line is a linear fit. Error bars indicate the statistical components of uncertainties (standard deviation, see text).

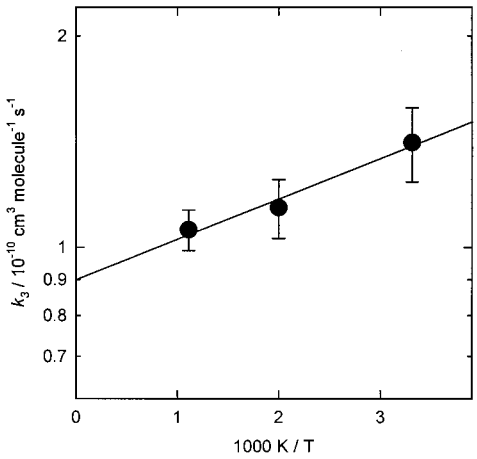

Figure 5. Temperature dependence of k_3 (determined at bath gas concentration [He] = 12.0×10^{16} molecules cm^3) in an Arrhenius form.

in the experiments lie in the range $(1.1-1.4) \times 10^{-10}$ cm^3 $molecule^{-1}$ s^{-1} ($T = 297-900K$). The rate constants display a weak negative temperature dependence (Figure 5) that can be represented with the Arrhenius expression

$$k_3 = (9.00 \pm 0.92) \times 10^{-11}\exp(57.4 \pm 19.1\ \mathrm{K}/T)\ \mathrm{cm^3\ molecule^{-1}\ s^{-1}} \quad \text{(II)}$$

Error limits in expression II represent uncertainties of the statistical fit only and are given as 2σ.

HCl was detected as a product of reaction 3 at 302 K. The growth time of HCl matched that of the $CHCl_2$ decay in the reaction with O. The other product of this channel of reaction 3, ClCO, could not be detected since it thermally decomposes with a rate exceeding 1000 s^{-1} at the pressures used in these experiments.[10] Attempts to detect other primary products of reaction 3 were unsuccessful. The following potential products were searched for CHClO, CCl_2O, HCO, and CCl_2. The absence of a measurable ion signal, however, cannot be taken as proof of the insignificance of these possible products in reaction 3 as sensitivity coefficients are not known for these species. A potential byproduct of the photolysis of dichloroacetyl chloride, CHCl, could form HCl as a product of its reaction with O atoms. However, experiments designed to detect CHCl among the products of the photolysis of $CHCl_2C(O)Cl$ (reaction 4) produced no measurable signal at the mass of CHCl (m/z = 48) at room temperature even with $CHCl_2C(O)Cl$ concentrations exceeding those used in experiments to measure k_3 by a factor of 10. Moreover, the CHCl signal was observed as a product of reaction 4 at 900 K, which indicates a sensitivity sufficient for detection of this species. Therefore, we interpret the observed HCl signal as that of a product of reaction 3.

Experimental Uncertainties. The sources of error in the measured experimental parameters such as temperature, pressure, flow rate, signal count, etc., were subdivided into statistical and systematic in nature. The uncertainties of the measured experimental parameters were propagated to the final value of the O atom concentration using different mathematical procedures for propagating systematic and statistical uncertainties.[11] The effects of variation of k_6 and k_7 values within their respective uncertainty limits on the fitted values of k' were included in the computation of the k' error limits, which were assumed to be statistical in nature. It can be seen from the k' vs $[O]_0$ plots in Figures 2-4 that the statistical uncertainties of individual experiments to measure k' are consistent with the extent of deviations of corresponding data points from the fitted line. Thus, the statistical contributions to the uncertainties of the final k_3 values at each temperature were obtained from the standard deviations of the linear fit of the k' vs [O] dependences. The error limits of the experimentally obtained k_3 values reported in Table 1 represent sums of the 2σ statistical uncertainty and the systematic uncertainty obtained from the average relative systematic uncertainty of $[O]_0$.

Tests were conducted to ensure that reaction 3 is the only process that can remove $CHCl_2$ radicals in the experimental system. In particular, special experiments were designed to demonstrate the absence of measurable reactions between $CHCl_2$ and SO or SO_2. These experiments were conducted under conditions of excess of $[CHCl_2]_0$ over $[SO]_0$ and $[O]_0$. High initial concentrations of $CHCl_2$ (an order of magnitude higher than those used in measurements of k_3) were employed. No differences could be detected between the SO_2 temporal profiles obtained in the presence or absence of $CHCl_2$ and other products of the $CHCl_2C(O)Cl$ photolysis. Similarly, no effects of the presence or absence of $CHCl_2C(O)Cl$ (and its photolysis products) on the signal profiles of SO could be detected at room temperature and at 500 K. However, at 900 K, a slow decay of SO ($6-20$ s^{-1}, depending on $[CHCl_2C(O)Cl]$) was observed in the presence of the products of $CHCl_2C(O)Cl$ photolysis. The rate of this decay was 10 times lower than the change in the rate of O atom decay due to the presence of $CHCl_2C(O)Cl$ photolysis products. Under the experimental conditions, several reactive processes could occur, including fast reactions of the $CHCl_2$ radicals with themselves and with other products of the $CHCl_2C(O)Cl$ photolysis. The observed slow decay of SO at 900 K can be attributed to a reaction between SO and a product of either the $CHCl_2C(O)Cl$ photodissociation or one of the above reactive processes. It is unlikely that this SO decay is caused by a reaction with $CHCl_2$ since SO has been shown to be quite unreactive with hydrocarbon and chlorine-substituted hydrocarbon radicals under conditions similar to those used in the current experiments (refs 4,5,7,8 and references therein). However, since the reaction between SO and $CHCl_2$ cannot be ruled out completely, we suggest an additional uncertainty of 10% in the direction of lowering the k_3 value at 900 K.

IV. Discussion

The work presented here is the first direct experimental determination of the rate constant of the reaction between the $CHCl_2$ radical and $O(^3P)$ atoms as a function of temperature. The weak negative temperature dependence obtained is similar

to that observed in other reactions of substituted methyl radicals with oxygen atoms.[4,5,7] The absolute values of the rate constants ($k_3 = (1.1-1.4) \times 10^{-10}$ cm^3 molecule^{-1} s^{-1} at $T = 297-900$ K) are between the values obtained earlier for the CH_2Cl ($k_2 = (1.5-2.7) \times 10^{-10}$ cm^3 molecule^{-1} s^{-1}) and CCl_3 ($k_1 = (0.27-0.44) \times 10^{-10}$ cm^3 molecule^{-1} s^{-1}) over similar temperature ranges. The apparent trend of a decrease in the R + O reaction rate constant with increasing Cl atom substitution does not carry through, however, to the case of unsubstituted methyl radical. The rate constant of the CH_3 + O reaction is equal to 1.4×10^{-10} cm^3 molecule^{-1} s^{-1} and is independent of temperature.[8,12]

The mechanism of reaction 3 is expected to proceed via the formation of a highly vibrationally excited (E > 368 kJ mol^{-1})[13] adduct, $CHCl_2O^*$, that instantly decomposes into further products. The recent quantum chemical study of Hou, Wang, and Gu[13] identified the three most likely channels of further decomposition of $CHCl_2O^*$:

$$CHCl_2 + O \rightarrow CHCl_2O^* \rightarrow Cl + CHClO(9.1 \text{ kJ mol}^{-1}) \quad (3a)$$

$$\rightarrow HCl + ClCO(33.0 \text{ kJ mol}^{-1}) \quad (3b)$$

$$\rightarrow H + CCl_2O(59.5 \text{ kJ mol}^{-1}) \quad (3c)$$

Energy barriers (values in parentheses) for the decomposition of $CHCl_2O$ via individual channels were obtained[13] in modified G2(MP2) calculations. The low values of these critical energies result in high values of *k(E)*, the microscopic energy-dependent rate constants of $CHCl_2O$ decomposition ($k(E = 368 \text{ kJ mol}^{-1}) \approx 10^{13}$ s^{-1}). Such high *k(E)* ensure the pressure independence of the overall reaction rate constant and channel distribution because stabilization cannot compete with decomposition at any experimentally accessible pressure. Hou, Wang, and Gu concluded that the lowest energy channel, 3a, is likely to be dominant, although channel 3b can be competitive.

The experimental results of the current work do not provide conclusive information on the channel distribution in reaction 3. Although HCl was detected as a primary product of reaction 3, a quantitative value of the corresponding channel (3b) yield could not be determined. The fact that no products of channels 3a (CHClO) and 3c (CCl_2O) could be detected cannot serve as a proof of their insignificance because of their unknown sensitivity coefficients (see above).

The relative importance of reaction channels 3a, 3b, and 3c can be approximately evaluated by comparing microscopic energy-dependent rates, *k(E)*, for each channel at the energy corresponding to the barrier for the decomposition of $CHCl_2O$ to O and $CHCl_2$ (the reverse of the "entrance" channel of this chemically activated reaction), 368 kJ mol^{-1}. RRKM theory provides the following formula for *k(E)*:[14,15]

$$k(E) = \frac{l^{\neq} W^{\neq}(E)}{h\rho(E)} \quad \text{(III)}$$

where $W^{\neq}(E)$, $\rho(E)$, and $l^{\neq}$ are the transition state sum-of-states and the active molecule density-of-states functions and the reaction degeneracy, respectively. Since the density-of-states function is the same for all three channels, the individual $l^{\neq}W^{\neq}(E)$ factors can be compared instead of the *k(E)* values.

Calculation of the $l^{\neq}W^{\neq}(E)$ factors was performed using the properties of the transition states from ref 13. The values of $l^{\neq}W^{\neq}(E = 368 \text{ kJ mol}^{-1})$ obtained for channels 3a, 3b, and 3c are comparable: ($9.2 \times 10^8/1.0 \times 10^9/5.9 \times 10^8$ if no overall rotations are included and $1.8 \times 10^{11}/2.4 \times 10^{11}/1.3 \times 10^{11}$ if one one-dimensional rotational degree of freedom is assumed to be active[14,15]). The existence of two optical isomers of transition states for reaction channels 3a and 3b was taken into account.[15,16] This computational exercise has only a qualitative meaning since the applicability of statistical theories of chemical reactions, such as RRKM, to processes that are as fast as the decomposition of the excited $CHCl_2O$ formed in the $CHCl_2$ + O reaction ($k(E) \approx 10^{13}$ s^{-1}) is highly doubtful. The decomposition of $CHCl_2O^*$ occurs on a time scale that is too short to allow for full randomization of energy. In this respect, comparing sums of states of the individual channel transition states may still be meaningful in spite of the fact that the RRKM formula for *k(E)* is not valid. This approach to the assessment of the relative importance of channels requires only a relaxed ergodicity assumption: that, in the transition states, all states of equal energy are reached with equal probability by the trajectories originating from the excited $CHCl_2O$ molecule. No assumption of a random energy redistribution within the molecule's phase space is required.

An additional uncertainty is introduced by the uncertainties of G2(MP2) values of reaction barriers and by the fact that the transition state for channel 3b could be found[13] only at the semiempirical level of calculations. The above discussion serves to demonstrate that no unequivocal conclusion regarding the distribution of products of reaction 3 can be derived from either the experimental data or from the results of quantum chemical calculations.

V. Conclusion

The rate constants of the reaction

$$CHCl_2 + O \rightarrow \text{products} \quad (3)$$

were determined in direct experiments using the Laser photolysis/photoionization mass spectrometry technique at low pressures of helium bath gas ([He] = 12.0×10^{16} molecules cm^{-3}). The values of the rate constants show a weak dependence on temperature over the 302−900 K range and can be represented by an Arrhenius expression $k_3(T) = (9.00 \pm 0.92) \times 10^{-11}\exp(57.4 \pm 19.1 \text{ K}/T)$ cm^3 molecule^{-1} s^{-1}. Rate constant values at individual temperatures (Table 1), when compared to the results of earlier studies of the reactions of other chloromethyl radicals with O atoms, demonstrate a trend of decreasing values of the R + O reaction rate constant upon increasing chlorination. This trend does not carry through, however, to the case of the unsubstituted methyl radical. HCl was detected as a product of the $CHCl_2 + O(^3P)$ reaction. No conclusion can be reached, however, on the relative importance of other potential products of reaction 3 on the basis of either experimental data or quantum chemical calculations.

Acknowledgment. This research was supported by the Division of Chemical Sciences, Office of Basic Energy Sciences, Office of Energy Research, U.S. Department of Energy under Grant DE-FG02-94ER1446.

References and Notes

(1) Knyazev, V. D.; Slagle, I. R. *J. Phys. Chem. A* **1998**, *102*, 1770.
(2) (a) Ho, W. P.; Yu, Q.-R.; Bozzelli, J. W. *Combust. Sci. Technol.* **1992**, *85*, 23. (b) Bozzelli, J. W. Private communication.
(3) Ryan, K. R.; Plumb, I. C. *Int. J. Chem. Kinet.* **1984**, *16*, 591.
(4) Seetula, J. A.; Slagle, I. R.; Gutman, D.; Senkan, S. M. *Chem. Phys. Lett.* **1996**, *252*, 299.
(5) Seetula, J. A.; Slagle, I. R. *Chem. Phys. Lett.* **1997**, *277*, 381.
(6) Slagle, I. R.; Gutman, D. *J. Am. Chem. Soc.* **1985**, *107*, 5342.

(7) Seetula, J. A.; Kalinovski, I. J.; Slagle, I. R.; Gutman, D. *Chem. Phys. Lett.* **1994**, *224*, 533.
(8) Slagle, I. R.; Sarzynski, D.; Gutman, D. *J. Phys. Chem.* **1987**, *91*, 4375.
(9) Krasnoperov, L. N.; Niiranen, J. T.; Gutman, D.; Melius, C. F.; Allendorf, M. D. *J. Phys. Chem.* **1995**, *99*, 14347.
(10) Nicovich, J. M.; Kreutter, K. D.; Wine, P. H. *J. Chem. Phys.* **1990**, *92*, 3539.
(11) Bevington, P. R. *Data Reduction and Error Analysis for the Physical Sciences*; McGraw-Hill: New York, 1969.
(12) Baulch, D. L.; Cobos, C. J.; Cox, R. A.; Esser, C.; Frank, P.; Just, Th.; Kerr, J. A.; Pilling, M. J.; Troe, J.; Walker, R. W.; Warnatz, J. *J. Phys. Chem. Ref. Data* **1992**, *21*, 411.
(13) Hou, H.; Wang, B.; Gu, Y. *J. Phys. Chem. A* **1999**, *103*, 8075.
(14) Robinson, P. J.; Holbrook, K. A. *Unimolecular Reactions*; Wiley-Interscience: New York, 1972.
(15) Gilbert, R. G.; Smith, S. C. *Theory of Unimolecular and Recombination Reactions*; Blackwell: Oxford, 1990.
(16) Karas, A. J.; Gilbert, R. G.; Collins, M. A. *Chem. Phys. Lett.* **1992**, *193*, 181.